

In-depth clinical characterization of intravenous iron infusion-induced hypophosphatemic osteomalacia and its resolution

Felix N. von Brackel , Jonathan Grambeck, Florian Barvencik, Michael Amling, Ralf Oheim* 

Department of Osteology and Biomechanics, University Medical Center Hamburg-Eppendorf, Lottestrasse 59, 22529 Hamburg, Germany

*Corresponding author: Ralf Oheim, Department of Osteology and Biomechanics, University Medical Center Hamburg-Eppendorf, Lottestrasse 59, 22529 Hamburg, Germany (r.oheim@uke.de).

Abstract

Iron deficiency anemia is treated by iron supplementation. Increasing evidence has shown that the carbohydrate components in iron infusions can cause hypophosphatemia and subsequent osteomalacia due to excess intact fibroblast growth factor 23 (iFGF23). We here undertook an in-depth characterization of 13 patients with iron infusion-induced osteomalacia (IIIO). Patients were characterized (monocentric institutional practice) by means of laboratory, bone density, HR-pQCT, and virtual osteoid volume estimation. We additionally report a patient who was treated with burosumab because iron infusions had to be continued despite osteomalacia. All 13 patients received ferric carboxymaltose (FCM) infusions and presented with low phosphate levels. Stopping the FCM infusions and supportive treatment by substitution of phosphate, calcium, native, and/or active Vitamin D was the chosen therapeutic approach. Pain, mobility, and biochemical data, such as serum phosphate levels, BMD, bone microstructure, and virtual osteoid volume, were the main outcome measures. Our results indicate biochemical normalization (eg, phosphate levels pre: $0.50 \text{ mmol/L} \pm 0.23 \text{ mmol/L}$, post: $0.93 \text{ mmol/L} \pm 0.32 \text{ mmol/L}$, $p < .001$) after stopping the FCM infusion and establishing supportive treatment. Additionally, pain levels on the visual analog scale (VAS) decreased ($\text{VAS}_{\text{pre}} 7.31 \pm 1.22$, $\text{VAS}_{\text{post}} 2.73 \pm 1.27$, $p < .0001$) and areal BMD (expressed by T-score) improved significantly ($\text{T-score}_{\text{pre}}: -1.85 \pm 1.84$, $\text{T-score}_{\text{post}}: -0.91 \pm 2.13$, $p < .05$). One patient requiring ongoing FCM infusions experienced significant additional benefits from burosumab treatment. In conclusion, our results highlight the importance of monitoring phosphate in patients treated with FCM infusions. Stopping FCM infusions is effective in addressing the excess of iFGF23 and thereby phosphate wasting. Supportive therapy enables quick recovery of the musculoskeletal system and improves pain levels in these patients.

Keywords: iron, osteomalacia, bone, HR-pQCT, FGF23, hypophosphatemia

Lay Summary

Iron infusions are important to treat iron deficiency anemia. Several case reports suggest that iron infusions lead to low phosphate levels (hypophosphatemia) that subsequently soften the bone tissue (osteomalacia), leading to pain and fractures. The proposed mechanism for the development of hypophosphatemia involves intact fibroblast growth factor 23 (iFGF23), a hormone that facilitates phosphate elimination through the kidneys. It is currently assumed that the carbohydrate components of iron infusions interfere with the degradation of iFGF23, resulting in its accumulation and subsequent renal phosphate loss. We present 13 patients that received iron infusions with subsequent phosphate wasting and osteomalacia evident by laboratory findings, low bone mass, and an increased incidence of fractures that occurred with no or minimal trauma. When stopping the infusions and treating the patients, the phosphate levels returned to normal and the bone mass increased significantly. Additionally, the patients had a significant pain relief, and their muscular performance increased. The treatment did consist of supplying phosphate and calcium tailored to the need as well as Vitamin D and active Vitamin D. One patient, that had to continue the iron infusions, was specifically treated with an iFGF23 antibody (burosumab). Taken together, it is important to monitor patient's phosphate levels to detect iron infusion-induced osteomalacia and to distinguish those from osteoporotic patients. Stopping the infusions and supplying supportive treatment is effective for recovering the musculoskeletal system of these patients.

Introduction

Iron deficiency is a common condition in clinical practice. In 2016, >40% of children, >40% of pregnant women, and >30% of nonpregnant women were anemic worldwide.¹ Addressing this high prevalence, the WHO is aiming to reduce it by 50% by 2025.^{1,2} Oral iron substitution is the first-line therapy and is effective in most cases.¹ However, for severe anemia, clinical symptoms, poor response to oral substitution, or adverse effects, parenteral iron substitution is used for intravenous iron infusions (III). In modern infusion therapy,

iron is encapsulated in a carbohydrate shell, delaying iron release and thereby reducing its toxicity.¹ Specifically, ferric carboxymaltose (FCM), ferric derisomaltose (FDI), and ferumoxytol create stable encapsulants for slow iron release.¹ These infusions are generally considered safe³ but are “associated with an increased risk of electrolyte disorder”, mostly hypophosphatemia (relative risk of 2.45), as stated in the respective package leaflets.^{3,4}

Since 2009, an increasing number of case reports have indicated that some patients who undergo intravenous iron

Received: July 10, 2024. Revised: October 25, 2024. Accepted: November 4, 2024

© The Author(s) 2024. Published by Oxford University Press on behalf of the American Society for Bone and Mineral Research.

This is an Open Access article distributed under the terms of the Creative Commons Attribution Non-Commercial License (<https://creativecommons.org/licenses/by-nc/4.0/>), which permits non-commercial re-use, distribution, and reproduction in any medium, provided the original work is properly cited. For commercial re-use, please contact journals.permissions@oup.com

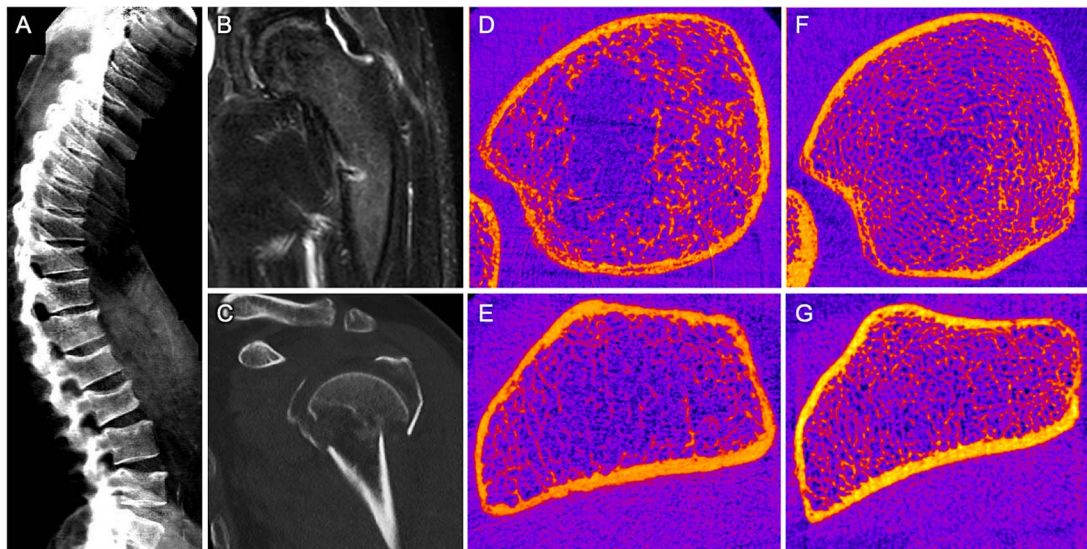


Figure 1. Potential skeletal manifestations of iron infusion-induced osteomalacia: multiple vertebral fractures in the VFA (A) may occur because of prolonged osteomalacia. Another manifestation may be pseudofracture, as evident in the MR images of one patient who was receiving III therapy (B), but fractures such as those of the proximal humerus may also occur after falls because of weakened bone (C). Bone microstructure may be affected, such as in the case of a tibia with irregular and coarse trabecularization (D) or a reduced trabecular network (E). For comparison, (F) and (G) depict the bone structure of a healthy, sex-matched young subject.

therapy develop osteomalacia following prolonged and excessive phosphate wasting.^{4–9} Specifically, FCM is associated with a significantly increased risk of hypophosphatemia.^{6,7} However, saccharated ferric oxide and iron polymaltose also pose a risk of hypophosphatemia, which can cause hypophosphatemic osteomalacia if persisting for a long time unrecognized and untreated. Clinically, these patients can present with vertebral fractures (Figure 1A), pseudofractures (Figure 1B), and insufficiency fractures in other skeletal regions (Figure 1C) attributed to decreased bone density by densitometric analysis^{7,9} and impaired bone structure (Figure 1D and E). For this reason, these patients can be incorrectly assumed to have a severe form of osteoporosis. Further symptoms include bone and muscle pain as well as weakness, fatigue, respiratory symptoms, nausea, vomiting, and diarrhea.¹⁰

Phosphate wasting is here mediated by an increase in the level of intact fibroblast growth factor 23 (iFGF23).^{4,5,10} Importantly, the production of the biologically active form, intact FGF23 (iFGF23), is generally increased in cases of iron deficiency anemia; however, under physiological conditions, elevated iFGF23 levels are inactivated by a likewise increased cleavage, thus iFGF23 levels remain within physiological levels.^{4,5} In the case of intravenous iron administration, the carbohydrate constituents of the iron supplement are discussed to suppress the iFGF23 cleavage and thereby its inactivation.

Inappropriately elevated levels of iFGF23, with respect to low serum phosphate levels, lead to increased and prolonged phosphate excretion via downregulation of the proximal tubule sodium phosphate cotransporters NaPi-2a and NaPi-2c.⁵ Additionally, iFGF23 suppresses the enzymatic Vitamin D activation by reducing CYP27B1 and increases the Vitamin D inactivation by enhancing CYP24A1. This leads, in addition to renal phosphate loss and chronic hypophosphatemia, to a disturbance of the calcium homeostasis.⁵ This process is sustained and reinforced due to often repetitive dosages of iron for the treatment of anemia. Therefore, anemia and

iron infusions act together in a vicious cycle leading to increased iFGF23 levels, causing renal phosphate loss, chronic hypophosphatemia, and subsequent osteomalacia.

The impact of uncoupled iFGF23 levels that are, with respect to the existent hypophosphatemia, inappropriately normal or elevated is also recognized in other diseases, such as X-linked hypophosphatemia (XLH) and tumor-induced osteomalacia (TIO). For these conditions, a monoclonal FGF23 antibody (burosumab) is available as a specific treatment option to reduce iFGF23 activity.

Clinical awareness is essential to address not only the necessity of monitoring phosphate levels after iron infusion but also to ensure appropriate treatment and to recognize iron infusion-induced osteomalacia (IIIO) as a potential differential diagnosis for patients with low BMD and/or (re)occurring fractures, especially in patients in whom iron deficiency is (repeatedly) treated by III.

Here, we aimed to characterize 13 patients diagnosed with intravenous iron-induced hypophosphatemic osteomalacia in depth, including clinical, biochemical, and microstructural parameters. We hypothesized that stopping iron infusions and supporting the supply of phosphate, calcium, Vitamin D, and active Vitamin D normalizes phosphate and calcium homeostasis, thereby treating osteomalacia and improving bone density and structure.

Materials and methods

Patient

Patients who presented between May 2016 and August 2023 at our outpatient clinic with musculoskeletal impairment of unknown cause were retrospectively selected. The diagnosis of intravenous iron-induced hypophosphatemic osteomalacia was initially established during the patient's first consultation at our outpatient clinic after a full clinical assessment was available. The term "first presentation" pertains to the initial visit to our outpatient clinic, during which low serum

phosphate levels were first identified. Patients with hypophosphatemic osteomalacia were included if iron infusion was given, and patients with differential diagnoses, such as hereditary forms of hypophosphatemia and chronic kidney diseases, were excluded. Hence, treatment with iron infusion was the primary cause for inclusion. Data was analyzed according to the rules of the local ethics committee of the University Medical Center Hamburg-Eppendorf, Germany. In addition, approval from the local ethics board of the state of Hamburg (Germany) was given (PV5364). This study was conducted in accordance with local laws and regulations and according to the Declaration of Helsinki. All patients provided written informed consent for retrospective data analysis. Pretreatment refers to the pretreatment at initial presentation, while post-treatment denotes the period following cessation or alteration of iron infusion therapy accompanied by our supportive therapy. The patient presented, treated with s.c. burosumab, provided written informed consent for this off-label therapeutic approach.

Clinical characteristics

The presence of fractures was assessed by means of a structured, clinical interview by an experienced physician, a visual inspection of the available image data, and a questionnaire. Furthermore, fractures were adjudicated by an experienced radiologist in conjunction with the clinical presentation and fracture history. Additionally, a vertebral fracture assessment (VFA) was carried out at the first consultation to check for unrecognized fractures of the vertebral bodies using a Lunar iDXA (GE Healthcare, Madison, WI, USA). Therefore, the patient was asked to lay on the side, preferably on the left, and the VFA was measured according to the manufacturer's recommendations. Pain levels were assessed using the visual analog scale at the time of the primary consultation and during treatment. The medical history was taken from the patient's files together with other important anamnestic data.

Biochemical assessment

Blood and urine samples were collected during clinical consultations in the daily routine. In case of doubt or borderline results, patients were invited to a second visit for a fasting morning blood sample. Samples were sent to our local laboratory (Institute for Clinical Chemistry and Laboratory Medicine, University Medical Center Hamburg, Germany). Serum samples from routine blood sampling were used to assess hemoglobin (Hb), red blood cells (Ery), calcium, phosphate, alkaline phosphatase (ALP), creatinine, bone-specific alkaline phosphatase (bAP), gamma-glutamyltransferase (GGT), osteocalcin, parathyroid hormone (PTH), 25-hydroxyvitamin D3 (25(OH)D₃), active Vitamin D (1,25(OH)₂D₃), and iFGF23 levels. Creatinine, calcium per creatinine (Ca/Crea), tubular phosphate reabsorption rate (TPR), and deoxyypyridinoline per creatinine (DPD/Crea) levels were routinely assessed using urine samples from the same day of consultation.

For specific parameters, dedicated test sets and machinery were used, as listed below. Serum parameters, including calcium, phosphate, creatinine, GGT, ALP, Vitamin D3 (25-OH-D₃), and PTH, as well as urine calcium and creatinine, were analyzed by an Atellica-Solution system (Siemens, Munich, Germany). For serum osteocalcin, active Vitamin D, iFGF23, and bAP, a Liaison XL Diasorin (Stillwater,

MN, USA) was used. The levels of DPD in urine were determined by an immune set from Immulite XP, Siemens, Munich, Germany. TPR was calculated using serum and urinary creatinine and phosphate by calculating $TPR = 100 \times (1 - (\text{phosphat}_{\text{urine}} \times \text{creatinine}_{\text{serum}}) / (\text{creatinine}_{\text{urine}} \times \text{phosphate}_{\text{serum}}))$. TmP/GFR (in $\%(\text{mmol/L})/(\text{mL/min})$) was calculated according to the following formula: $(P \times TPR) / \text{GFR}$.

DXA: areal BMD (aBMD)

The areal BMD (aBMD) was assessed during routine clinical examinations according to the ISCD.¹¹ Density measurements were carried out via Lunar iDXA (GE Healthcare, Madison, WI, USA). Scans were performed at the lumbar spine (L1-L4) and both hips. The lowest T-score was determined by selecting the lowest T-score among at least two adjacent vertebral bodies, the total hip or femoral neck. The determination of the highest T-score was selected by following a similar approach. T-scores were calculated by the manufacturer's software. Based on the lowest T-scores and according to the densitometric WHO definition, 9 out of 13 patients were categorized as having osteoporosis, 3 as having osteopenia, and 1 as having BMD within the reference range.

High-resolution peripheral quantitative computed tomography (HR-pQCT)

HR-pQCT (XtremeCT I and II, Scanco Medical, Brüttisellen, Switzerland) was routinely used to image the patient's bone microarchitecture and volumetric BMD. Here, the distal radius and distal tibia were scanned according to previously published guidelines.¹² The parameters quantified were the total volumetric BMD (Tt.vBMD), bone volume-to-tissue volume ratio (BV/TV), cortical thickness (Ct.Th), and trabecular thickness (Tb.Th), each for the radius and tibia. All images were checked for motion artifacts and were excluded if motion grading was >3 .¹³ By using the results of Manske *et al.*, parameters derived from the second generation of HR-pQCT (XtremeCT II) were recalculated¹⁴ to fit the first generation (XtremeCT I). Next, the percentage was computed relative to a comparison group from Burt *et al.* matched for age and sex.¹⁵ The percentage values of the BV/TV in relation to a reference group were determined according to the reference cohort of Hansen *et al.*¹⁶ since BV/TV was not reported by Burt *et al.*

Grip strength and chair rising assessment

Grip strength was assessed using a handheld dynamometer (Leonardo Mechanograph GF, Novotec Medical, Pforzheim, Germany) on a routine basis. Patients were seated with their arms resting at their legs. Subsequently, they were asked to repeat three cycles of grip strength assessment per side. The lowest and highest values of these six measures were selected for further statistical analysis.

The chair rising test (CRT) was performed on a Leonardo Mechanograph (GRFP STD, Novotec Medical, Pforzheim, Germany). Therefore, patients were asked to sit calmly on a bench and await a signal, after which they were supposed to stand up and sit down again for five cycles as rapidly as possible, ensuring full leg elongation when standing. A force reaction plate was used to record the maximum power per kilogram of body weight.

Table 1. Demographics: demographics at first presentation are listed, as well as the follow-up time, fracture occurrence, and pain levels.

Parameter	Unit	Iron infusion	
		Mean	SD
<i>n</i>	#	13	-
Age	yr	53	13
Sex (m:f)		9:4	-
Height	m	1.745	0.090
Weight	kg	72.26	23.56
BMI	kg/m ²	23.41	6.25
Vertebral #	%	6/13	-
Nonvertebral #	%	3/13	-
Mean FU time HR-pQCT	mo	16.00	4.90
Mean FU time Lab	mo	4.92	3.69
Mean FU time DXA	mo	13.25	7.13

Abbreviations: BMI, body mass index; FU, follow-up; Lab, laboratory; DXA, dual-energy absorptiometry; m, male; f, female; #, fracture.

Statistical evaluation

The groups were tested for a normal distribution first and subsequently compared according to the results of parametric Student's *t*-test in the case of a normal distribution and nonparametric tests in the case of a non-normal distribution. Specifically, paired testing was conducted if sufficient paired datasets (>5) were available. In this case, paired *t*-tests were used for normally distributed data, and Wilcoxon tests were used for normally distributed data if the data were not normally distributed in one of the two compared groups. A *p*-value <.05 was considered to indicate statistical significance. Tests were carried out using GraphPad Prism (v9.0.2, GraphPad Software LLC, California, United States).

Results

Patient characteristics

Thirteen patients with a mean age of 53 ± 13 yr were included in this study, 9 of whom were men. A total of 46.16% (6/13) had vertebral fractures, and 23.07% (3/13) had nonvertebral fractures. All clinical characteristics are listed in Table 1. The mean pain level at first presentation was 7.31 ± 1.22, which was significantly higher than in the follow-up after stopping or changing the III and adding supportive therapy (2.73 ± 1.27, *p*<.0001). Detailed information for each patient is given in Table S1.

All patients received an agent containing FCM at the first consultation. The mean time of receiving repetitive infusions was 4.7 yr ± 4.2 yr (min: 0.2 yr, max: 11 yr). The reasons for iron infusion were anemia of unknown origin in 3 patients, anemia caused by complications of (chronic) gastrointestinal diseases in 7 patients, and anemia caused by hereditary hemorrhagic telangiectasia (HHT) in 3 patients (for detailed information, see Table S1).

Ten patients were able to stop and/or switch to oral supplements directly after diagnosis and consultation with the prescribing doctor; 2 patients switched to FDI, but 1 patient had to remain on FCM infusions, as described in detail below. Five patients received bone-active drugs, all of whom were assumed to have osteoporosis prior to first presentation. Four patients were treated with antiresorptive drugs (2 patients received intravenous ibrandronic acid 3 mg every 3 mo for 1 yr, 1 patient received risedronic acid for 3 mo, and 2 patients

received a single injection of denosumab (one of them received ibrandronic acid before)), and one additional patient received teriparatide for 3 mo prior to the diagnosis of III/O.

The individual treatment consisted of native Vitamin D in all patients, active Vitamin D (1,25(OH)₂D₃) in 6/13 patients, calcium supplementation in 10/13 patients, and phosphate supplementation in 11/13 patients. Specifically, the mean daily dose of calcium was 458.8 mg ± 331.5 mg (min: 300 mg, max: 1200 mg), that of phosphate was 1725.3 mg ± 1122.8 mg (min: 612.2 mg, max: 3673.2 mg), and that of active Vitamin D (1,25(OH)₂D₃) was 0.35 μg ± 0.224 μg (min: 0.25 μg, max: 0.75 μg). The mean weekly dose of native Vitamin D was 32 857 IU/wk ± 15 313 IU (min: 8333 IU, max: 60000 IU). In 12 out of 13 patients, stopping the iron infusion or switching to another agent was the main approach in addition to symptomatic treatment, as described above. Treatment was patient-tailored and thus adapted during treatment, according to serum calcium, phosphate, PTH, and ALP levels.

One patient with Crohn's disease was not able to stop or switch FCM iron infusions due to an allergy to the substitutes or a poor response to other medications (thus not increasing or even decreasing ferritin serum levels). Therefore, FCM had to be continued, but iron sucrose (Venofer, iron(III)hydroxide-sucrose complex), blood transfusions, and erythropoietin were also applied, depending on Hb levels (Figure S1). During the treatment, burosumab was administered at an external clinic for a period of 5 mo 2-8 wk tailored to the serum phosphate level, as depicted in Figure S1. Administration had to be stopped due to hyperphosphatemia after 5 mo and re-administered for 6 mo according to the same application scheme.

Laboratory assessment

At first presentation, the mean phosphate level was 0.50 mmol/L ± 0.23 mmol/L and increased significantly over the course of treatment to 0.93 mmol/L ± 0.32 mmol/L (*p*<.001). Calcium levels remained constant (first presentation: 2.26 mmol/l ± 0.14 mmol/l, follow-up: 2.29 mmol/L ± 0.16 mmol/L, *p* = .20). The iFGF23 concentration significantly (*p*<.05) decreased from 274.3 pg/mL ± 455.90 pg/mL to 85.79 pg/mL ± 72.82 pg/mL, and TPR increased significantly (*p*<.05) from 85% ± 13% to 93% ± 52%, as well as TmP/GFR (in %(mmol/L)/(mL/min)) from 0.34 ± 0.24 to 0.94 ± 0.50 (*p*<.05). The concentration of active Vitamin D also significantly (*p*<.01) increased over the course of treatment from 38.67 ng/L ± 25.61 ng/L to 67.78 ng/L ± 26.17 ng/L. No significant changes in PTH or 25-OH-D3 serum levels were detected. The average levels of Hb and Ery, which are markers for anemia, were below the reference range at the initial presentation (Hb: 12.39 g/dL ± 2.4 g/dL, Ery: 4.26 × 10⁹/mL ± 0.67 × 10⁹/mL). Bone resorption did not differ between the two time points; however, the level of osteocalcin (BGLAP) increased significantly (*p*<.01) from 18.32 μg/L ± 7.78 μg/L to 34.50 μg/L ± 32.35 μg/L. Bone-specific ALP and ALP both significantly (*p*<.01) decreased from 45.76 μg/L ± 31.63 μg/L to 31.58 μg/L ± 28.83 μg/L and from 196.3 U/L ± 108.8 to 144.6 U/L ± 105.4 U/L, respectively (Figure 2).

Clinical assessment

aBMD measurements revealed a significant increase in aBMD for both the minimal T-score (first: -2.91 ± 1.01, follow-up: -2.38 ± 1.01, *p*<.05) and maximal T-score (first:

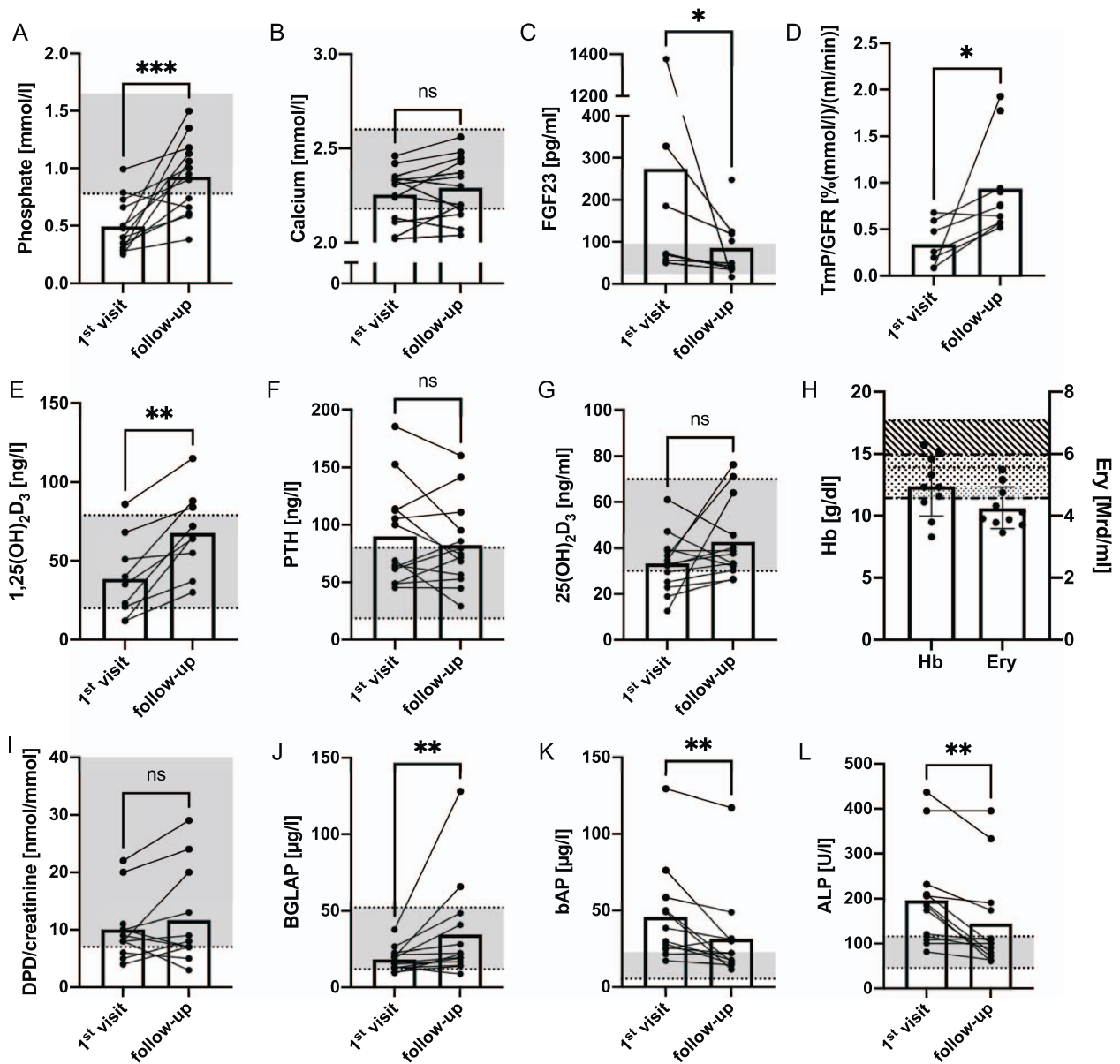


Figure 2. Laboratory assessment: significant improvements in the phosphate and iFGF23 levels (A, C) as well as the tubular phosphate reabsorption level (D) were detected, while no differences in the calcium level were detected (B). 1,25(OH)₂D₃ increased over the course of therapy (E), while mean PTH levels and Vitamin D remained unchanged (E, G). Serum hemoglobin and erythrocyte levels indicate anemia in patients at initial presentation (H). There were no differences in bone resorption (I), but increased bone formation (J) and decreased bAP and ALP levels (K, L) over the course of treatment. Abbreviations: ALP, alkaline phosphatase; BALP, bone-specific alkaline phosphatase; BGLAP, osteocalcin; 25(OH)₂D₃, 25-hydroxyvitamin D₃/Vitamin D; 1,25(OH)₂D₃, active Vitamin D; PTH, parathyroid hormone; TmP/GFR, tubular maximum for phosphate reabsorption per glomerular filtration rate; DPD, deoxypyridinoline; Hb, hemoglobin; Ery, erythrocytes; ns, not significant; **p*<.05; ***p*<.005; ****p*<.001.

–1.85 ± 1.84, follow-up: –0.91 ± 2.13, *p*<.05) selected from pooled DXA measurements of the lumbar spine and hip, as depicted in Figure 3A and B. Assessment of the muscle power revealed greater values for patients after treatment (17.17 mo ± 6.05 mo) than for patients before treatment (5.23 W/kg ± 2.34 W/kg, after 8.65 W/kg ± 0.76 W/kg, *p*<.005, Figure 3C), but the time per repetition did not differ between the two time points. The quantification of maximum grip strength revealed significantly higher values in follow-up (*p*<.005), and a tendency toward higher mean values was measured for minimal grip strength (*p*=.0678) after treatment (Figure 3D). The maximum grip force significantly increased during therapy for all patients who were available for paired testing (Figure 3E; first: 27.38 kg ± 11.11 kg

vs 31.18 ± 13.37, *p*<.05). The pain levels decreased 2.57-fold from 7.31 ± 1.22 (min = 5, max = 9.5) to 2.71 ± 1.27 (min = 1.5, max = 5.0), with a *p*-value <.0001 (Figure 3F). The DXA-based virtual osteoid volume was calculated using the spinal T-score instead of the spinal Z-score, according to Schmidt et al.¹⁷ The mean value was 24.63 ± 16.22 for the first measurement, which decreased significantly during the course of treatment to 17.22 ± 16.32 (*p* = .015).

Bone structure and 3D density (HR-pQCT)

HR-pQCT measurements generally indicated values below the reference values (Figure 4A), where women tended to have lower mean values than men did (Figure 4A). Notably, the percentage of total BMD (Tt.vBMD) relative to normative

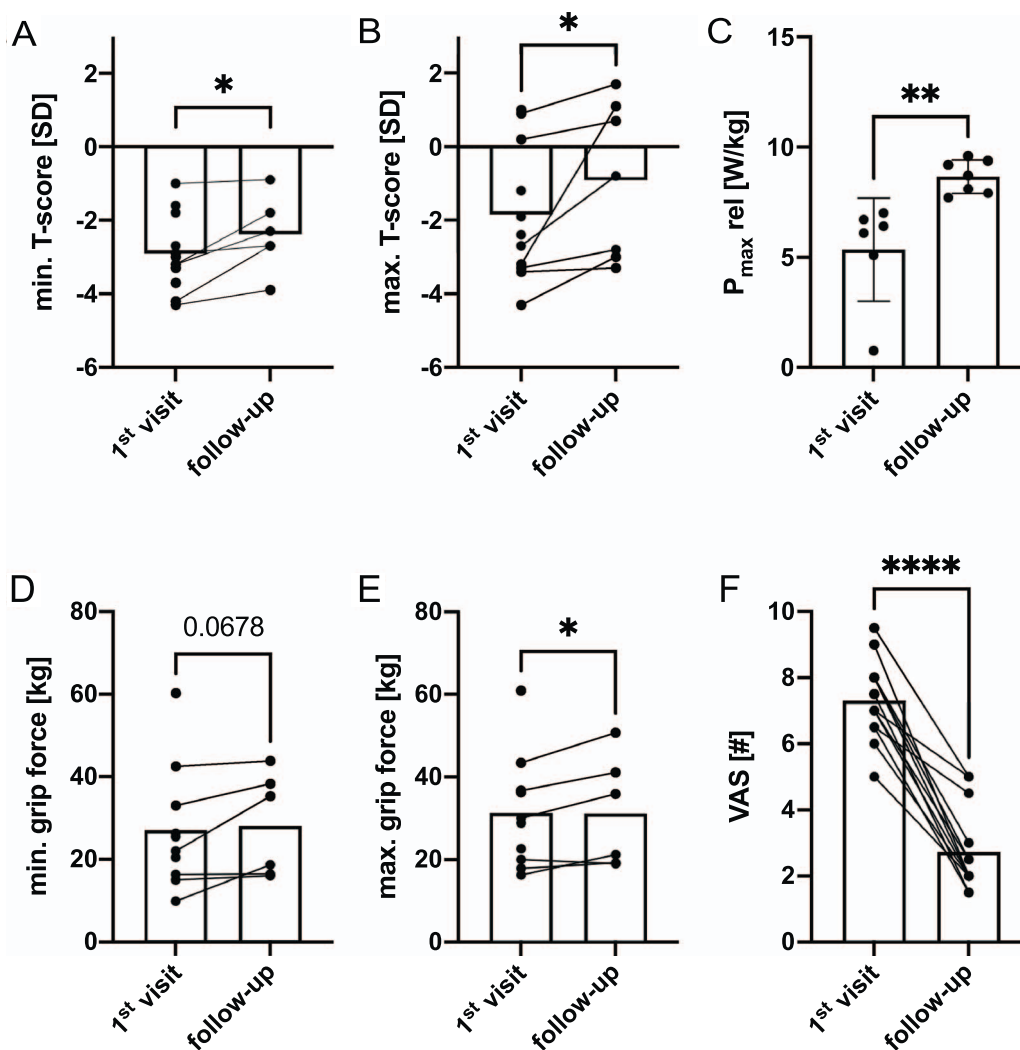


Figure 3. Clinical assessment: the minimal and maximal BMD determined from pooled lumbar and hip measurements increased significantly over the course of treatment (A, B). Furthermore, muscle performance was greater in patients after treatment than at first presentation (C). A tendency toward increased minimal grip strength was observed (D), as was a significant increase in maximum grip strength (E). Pain levels decreased significantly over the course of treatment (F). Abbreviations: Max., maximal; Min., minimal; VAS, visual analog scale; * $p < .05$; ** $p < .005$; **** $p < .0001$.

data was significantly higher in the radius compared to the tibia (radius: $87.33\% \pm 26.97\%$ vs tibia: $73.12\% \pm 25.80\%$, $p < .05$), indicating that vBMD values in the radius were closer to normal than those in the tibia. (Figure 4B). Similarly, although both were clearly below the reference values, the cortical thickness of the tibia was significantly lower than that of the radius (radius: $73.41\% \pm 23.68\%$ vs tibia: $63.44\% \pm 25.37\%$, $p < .05$, Figure 4C), based on percentages calculated for each patient relative to the mean reference data. Calculated according to Schmidt *et al.*,¹⁷ the HR-pQCT-based mean virtual osteoid volume decreased significantly from 23.14 ± 15.26 for the first measurement to 15.48 ± 9.06 for the second measurement ($p < .05$, Figure 4D).

Case presentation involving burosumab treatment

A 50-yr-old male patient receiving continuous FCM infusions because of chronic anemia as a result of Crohn's disease presented with severe hypophosphatemic osteomalacia with immobilization in a wheelchair. Symptomatic treatment consisted of 100 000 IU of Vitamin D every 3 wk as well as 1200 mg of supplemented calcium daily in combination

with $0.25 \mu\text{g}$ of alfacalcidol and 1224.4 mg of phosphate daily. This supportive treatment led to an increase in the spinal T-score from -2.7 to -0.8 and the lowest hip T-score from -4.2 to -2.7 (Figure 5E). The concentration of bone-specific ALP decreased over the course of this treatment from 145 to $22.9 \mu\text{g/L}$, and the DPD/creatinine ratio decreased from 20 to 4 nmol/mmol. 3D imaging of the radial and tibial bone structure and density revealed a distinct pattern (Figure 5A-D). Specifically, no changes in the radius were detected, but drastic improvements were detected in the tibia. Specifically, BV/TV increased by 280%, from 3.5% to 9.1% (+5.6%), and Tt.vBMD increased by 110.84%, from 91.2 to 192.1 mgHA/ccm (+100.9 mgHA/ccm, Figure 5A). The cortical thickness was 0.40 mm at the first measurement and 0.81 mm (+0.41 mm) at the follow-up, indicating an increase of 102.5%. The same pattern was observed for the trabecular thickness (0.032 mm to 0.058 mm, (+0.026 mm); Figure 5C). Interestingly, most of this increase was observed in the first year of treatment (between the first and second measurements), with a plateau between the second and third measurements. The improvement in skeletal parameters was

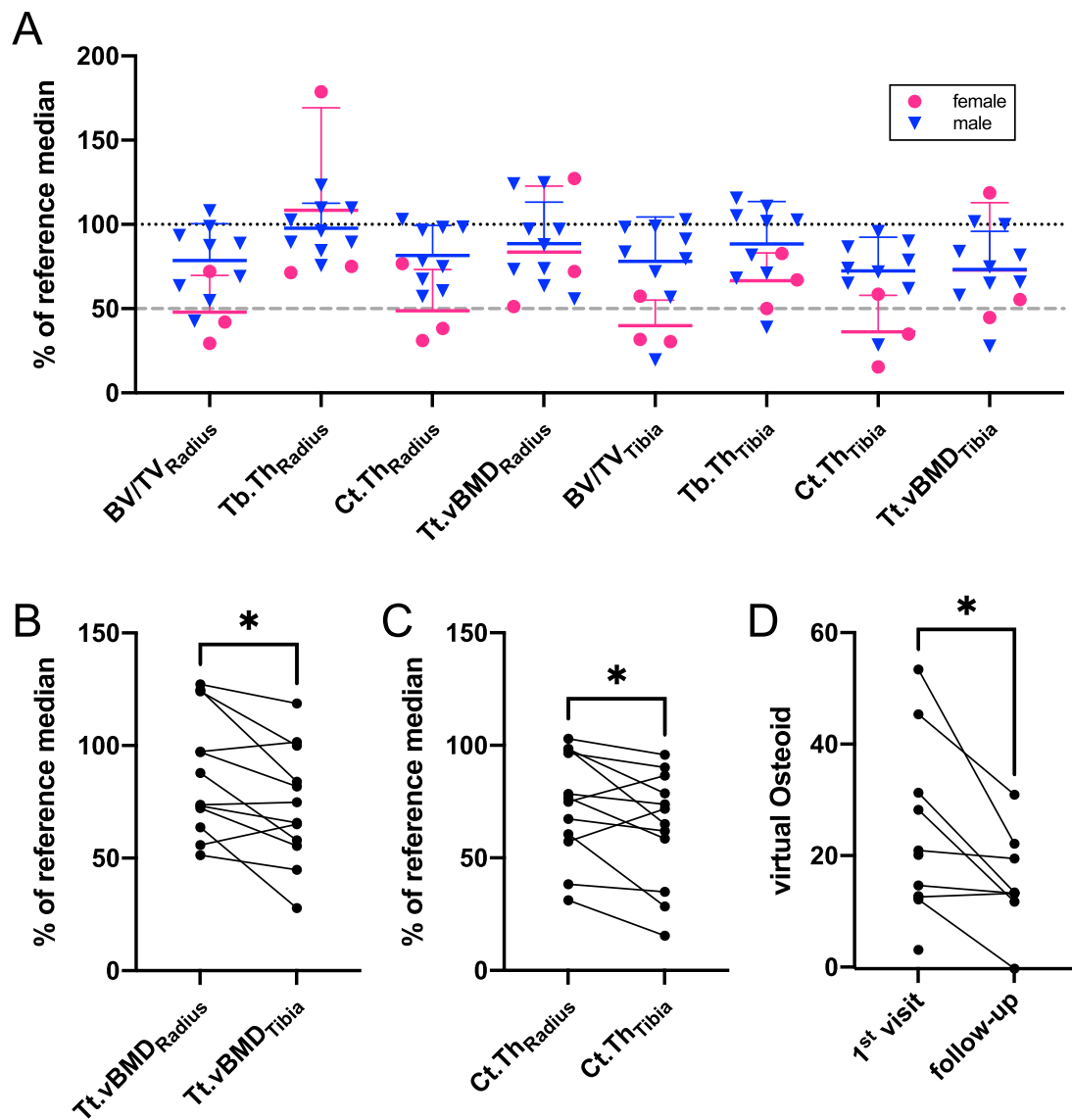


Figure 4. High-resolution peripheral quantitative computed tomography: parameters in percent of an age- and sex-matched reference group. The dotted, black line represents the mean (100%) of the reference group for comparison; the dashed, gray line represents 50%. Women (red/ circles) exhibited particularly low values compared to the reference group in bone microstructure and density (A) than men did (blue/ triangles). Interestingly, Tt.vBMD (B) and cortical thickness (C) were significantly greater in the tibia than in the radius. The virtual osteoid volume to bone volume ratio was calculated according to Schmidt *et al.*¹⁷ (here, based on DXA and ALP levels), exhibiting significantly lower osteoid volumes in the follow-up measurement after treatment (D). Abbreviations: Tt.vBMD, total volumetric BMD; BV/TV, bone volume to tissue volume; Tb.Th, trabecular thickness; Ct.Th, cortical thickness; FU, follow-up; 1st pres., first clinical consultation; * $p < .05$.

accompanied by strong improvements in muscle function with increasing mobility and a 67.97% increase in p_{max} in the CRT.

Subsequently, during this plateau phase, burosumab was administered off-label at an external clinic due to persistently very low serum phosphate, which was tailored to laboratory values of 30 mg s.c. (0.4 mg/kg body weight) every 6-8 wk from June 2023 to February 2024. A comparison of the imaging parameters prior to burosumab and post-burosumab treatment (at the time point of hyperphosphatemia, Figure S1) revealed an additional strong improvement in the tibial microstructure in terms of a +34.07% BV/TV (+3.1%), +29% Tt.vBMD (+55.7 mgHA/ccm), +55.56% Ct.Th (+0.45 mm), and +36.21% Tb.Th (+0.021 mm), comparable to the changes achieved by the supportive treatment prior to the plateau phase. No such changes were detected in the radius

(Figure 5B and D). Densitometric results at the spine and hip mirrored the results of the tibia, with a T-score increase at the lumbar spine from -0.8 to +0.6 and from -2.7 to -1.9 for the lowest hip T-score, respectively.

Discussion

Intravenous iron-induced osteomalacia (IIIO), resulting from unphysiologically elevated iFGF23 levels despite the presence of hypophosphatemia, has increasingly come into focus as a significant concern for clinicians and researchers. However, in international literature, this is primarily case report or review-based.^{7,18} In clinical practice, this rare side effect can easily be confused with osteoporosis since severe osteomalacia can also lead to low BMD and multiple (insufficiency) fractures (Figure 1). This confusion was also present in our cohort, as

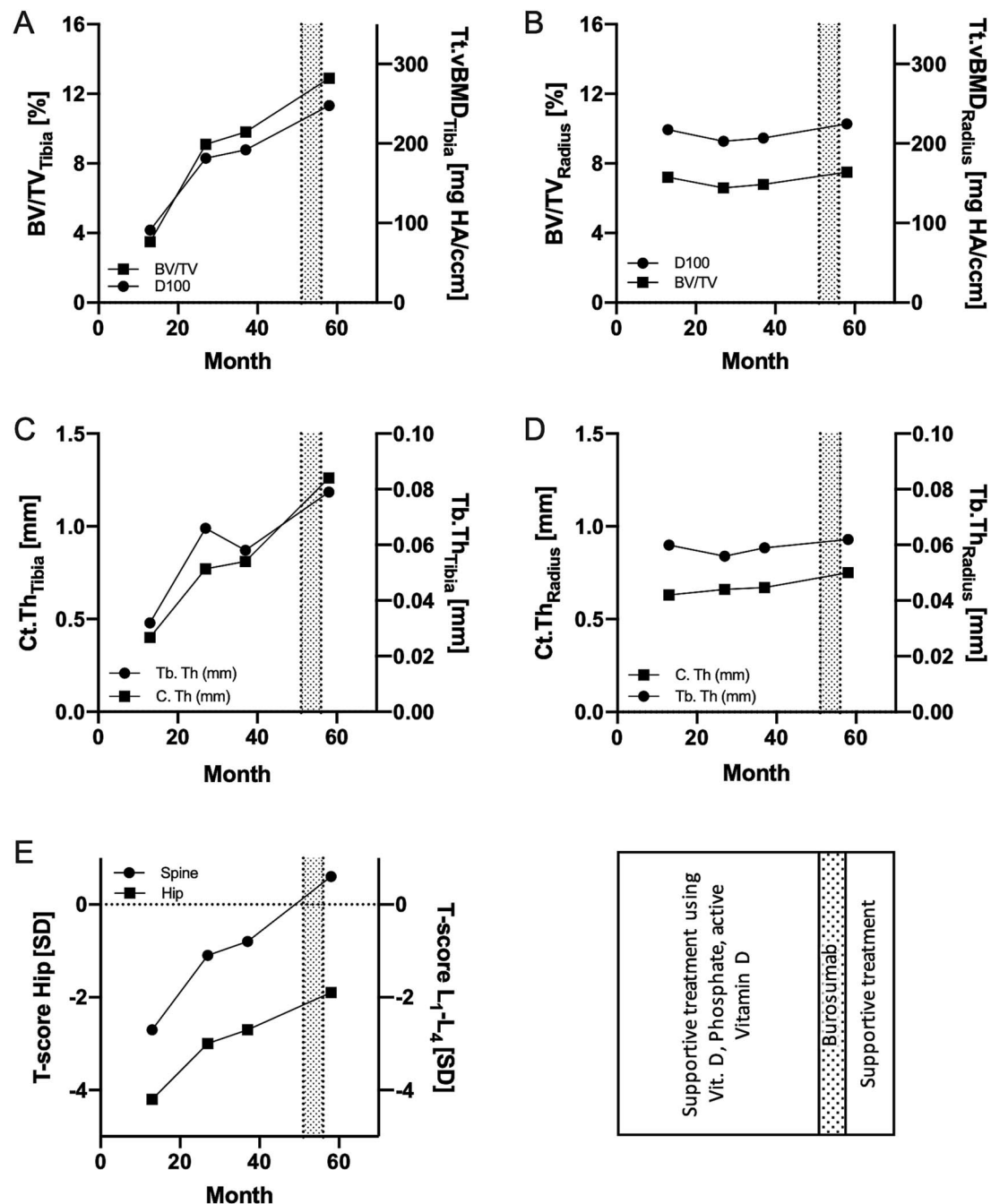


Figure 5. Clinical case with continued FCM infusions involving burosumab treatment: one patient had to continue FCM treatment due to allergic reactions or nonresponse to other infusions. Symptomatic treatment was carried out, improving bone structure and density significantly (A-E). However, a plateau was reached after 2 yr of treatment (measurements 2-3, A, C, and E). Importantly, the bone structure increased only in the load-bearing tibia (A vs B, C vs D), but the bone density improved in the hip and spine (E). Subsequent burosumab treatment had an additional effect on bone structure and density. Notably, the skeletal improvement in response to burosumab treatment was significant in terms of the tibial bone density and structure as well as the bone density at the hip and spine, but again not at the radius (B, D). Abbreviations: Tt.vBMD = Total volumetric BMD = D100, BV/TV = bone volume to tissue volume, Tb.Th = trabecular thickness, Ct.Th = cortical thickness, SD = standard deviation.

evidenced by multiple fractures being recorded and 5 of 13 patients being treated for osteoporosis prior to being correctly diagnosed with IIIO using bone-specific treatments. However, in cases of IIIO, such treatments may increase the risk of pseudofractures, emphasizing the need to address calcium and phosphorus metabolism before establishing osteoporosis treatments.

In our cohort, III were given due to anemia of unknown cause or secondary anemia caused by complications of chronic

bowel disease or HHT.¹⁰ While some gastrointestinal diseases may additionally aggravate osteomalacia through malabsorption, III was the main cause of osteomalacia, as indicated by the improvements after stopping the iron infusions. IIIO was evidenced by low serum phosphate levels as well as (relatively) high iFGF23 levels and elevated ALP as well as bone-specific ALP levels (Figure 2). All patients reported here received FCM infusions, which are known to cause hypophosphatemia particularly often. These results are in line with the literature

and mirror the effect of FCM infusion-induced phosphate wasting via iFGF23, as described before.^{6,10}

The specific pattern of hypophosphatemia and increased ALP (Figure 2) stresses the importance of phosphate monitoring during and after III to monitor possible interactions between phosphate metabolism and iron infusion agents. In addition, such measurements are generally crucial in patients with suspected bone diseases, such as osteoporosis, in order to rule out osteomalacia as an important differential diagnosis.

Anemia is known to induce FGF23 production via hypoxia-inducible factor (HIF-1 α).⁵ Under physiological conditions, iFGF23 is immediately cleaved and thereby inactivated. However, the constituents of iron infusions are known to interfere with this cleavage^{4,5} leading to increased iFGF23 levels (Figure 2), which causes renal phosphate loss and thereby hypophosphatemia and subsequently osteomalacia. This pathomechanism is in line with our findings, although some patients included here exhibited iFGF23 levels within the reference range. This could be explained by the rapid decrease of iFGF23 already several days after infusion.¹⁰ In addition, the iFGF23 level has to be interpreted in the context of the serum phosphate level since in (severe) hypophosphatemia iFGF23 should be suppressed under physiological conditions. Thus, iFGF23 levels in the upper normal range in hypophosphatemic patients do also represent a pathological finding.

Therefore, significantly increasing phosphate levels and lower iFGF23 and ALP levels after the cessation of FCM infusions clearly indicate its causative nature. Thus, stopping (or changing) the iron agent is of central importance for treating IIIO. In addition, supportive therapy is also necessary to enable fast recovery by restoring the phosphate and calcium homeostasis. Here, we used phosphate and active Vitamin D supplementation to counteract the effects of iFGF23. Additionally, native Vitamin D was given on a regular basis to prevent insufficiencies and calcium in the case of elevated PTH levels to account for the imbalanced calcium homeostasis. Both calcium and phosphate must be balanced since they form the bone mineral hydroxyapatite phase^{19,20} and thus affect the density and rigidity of bone. Phosphate supplementation was discontinued once the normalization of serum phosphate levels was achieved following the cessation of FCM infusion to mitigate potential side effects such as gastrointestinal complications or nephrocalcinosis. Calcium substitution treatment was maintained for a longer period to address the need for calcium along with the osteomalacia caused by the hungry bone syndrome.

Osteomalacia caused by III-induced hypophosphatemia yielded distinctly low T-scores (Figure 3). A total of 9/13 patients could be densitometrically classified within the osteoporotic range according to the WHO. Compared to the findings of Vilaca *et al.*, the presence of densitometric osteoporosis (Vilaca *et al.*: 53.3% vs here: 69.2%) and decreased BMD (Vilaca *et al.*: 68.8% vs here: 92.3%) were in our cohort especially pronounced. Given this observation and considering the multiple fractures, it becomes evident why osteoporosis treatment was chosen in some of the patients. But T-scores significantly increased after supportive treatment, as described above, within a short follow-up period (Table 1, Figure 3), indicating the great potential of restoring phosphate and calcium homeostasis and thereby bone mineralization. The presence of increased osteoid volumes was shown by virtual estimation using DXA and HR-pQCT parameters combined with ALP levels according to our previously

reported protocol.¹⁷ Furthermore, the general constitution of the patients vastly improved, as indicated by both a gain in muscular performance and a significant decrease in perceived pain (Figure 3), which is known for patients diagnosed with IIIO.^{5,8,10}

Notably, the effect on the peripheral skeleton was site-specific according to the HR-pQCT measurements. A significantly greater reduction in density and structure was detected in the tibia than in the radius (Figure 4). These results are in line with data from patients with tumor-induced osteomalacia, which are also more severely affected at the tibia than the radius.¹⁷ Virtual osteoid estimation using HR-pQCT and DXA revealed decreased osteoid volume in follow-up measurements. These results match the histological results showing that other iFGF23-mediated types of osteomalacia decreased after the excess iFGF23 was addressed.^{21,22}

In one patient, FCM injections could not be discontinued (Table S1) due to allergy or nonresponse to other agents. However, even in the case of ongoing FCM infusions, supportive therapy, including phosphate, calcium, and Vitamin D, helped to markedly decrease ALP levels and increase BMD in the spine and hip (Figures 2 and 5). Here again, the HR-pQCT measurements revealed improvements in the bone volume, density, and structure of the tibia but not the radius (Figure 5), indicating prior manifestation in skeletal regions with loading.

Between the first and second follow-up measurements, the bone densitometric and HR-pQCT parameters tended to plateau, indicating a balance between supportive therapy and continuous iFGF23 excess. Furthermore, the patient complained about persisting pain and restricted mobility after initial improvement. To address these concerns, the patient received off-label treatment with the FGF23 antibody burosumab to limit phosphate wasting and thereby hypophosphatemia and osteomalacia. Interestingly, there was an increase in phosphate serum levels as well as a significant and similar additional increase in bone mass, density, and structure under this treatment (Figure 5). This finding aligns with observations in other iFGF23-mediated phosphate loss syndromes, such as TIO,²² as well as a case report by Amarnani *et al.*, in which a severely affected IIIO patient was treated with burosumab (0.3 mg/kg every 2-8 wk) after the occurrence of multiple (pseudo)fractures.²³

This case illustrates both the effectiveness and limitations of the supportive therapy if the causative III cannot be stopped or replaced. Here, the FGF23 antibody burosumab effectively improved bone density and structure. In addition, phosphate and active Vitamin D supplementation administered several times a day could be omitted, improving the patients' overall wellbeing.

This study has several limitations, such as a limited number of patients ($n=13$) and the retrospective study design causing variations in the follow-up period and treatment adherence. Nevertheless, this is the largest cohort of IIIO patients published to date presenting real-world data from clinical practice, including the challenges in the diagnosis and management of such patients.

Conclusion

In conclusion, the occurrence of (pseudo) fractures and low BMD in patients with anemia and III should lead to the differential diagnosis of IIIO. In the case of suspected iron infusion-induced hypophosphatemia, phosphate and ALP

levels should be monitored, and iron infusion therapy should be adjusted to oral or other formulations or, if possible, discontinued. Moreover, phosphate and calcium loss should be addressed by phosphate and calcium substitution (to account for the large volumes of osteoid needed for mineralization) as well as by active and native Vitamin D substitution. This approach effectively normalizes not only laboratory results but also improves bone density and structure and decreases pain levels. Furthermore, phosphate testing should be a routine approach for screening patients suspected of having osteoporosis to address the potential differential diagnosis of iFGF23-mediated and other forms of osteomalacia.

Author contributions

Felix N. von Brackel (Data curation, Formal analysis, Investigation, Methodology, Software, Validation, Visualization, Writing—original draft, Writing—review & editing), Jonathan Grambeck (Data curation, Investigation, Methodology, Validation, Writing—review & editing), Florian Barvencik (Writing—review & editing), Michael Amling (Resources, Writing—review & editing), and Ralf Oheim (Conceptualization, Data curation, Methodology, Project administration, Resources, Supervision, Validation, Writing—review & editing).

Supplementary material

Supplementary material is available at *JBMR Plus* online.

Funding

FNvB was supported by the German Research Foundation (DFG) under Grant No. 499533307.

Conflicts of interest

F.N.v.B., J.G., and M.A. have no conflicts of interest. F.B. has received speaker fees from Alexion, UCB, and Diasorin and has received institutional research grants from UCB and Alexion. R.O. has served as a speaker and advisory board member for Kyowa Kirin, Inozyme, Ipsen, Pharmacosmos, UCB, and Mereo and has received an institutional research grant from Kyowa Kirin, UCB, and Inozyme.

Data availability

Restrictions apply to the availability of some or all data generated or analyzed during this study to preserve patient confidentiality or because they were used under license. The corresponding author will on request detail the restrictions and any conditions under which access to some data may be provided.

References

- Pasricha S-R, Tye-Din J, Muckenthaler MU, Swinkels DW. Iron deficiency. *Lancet*. 2021;397(10270):233–248. [https://doi.org/10.1016/S0140-6736\(20\)32594-0](https://doi.org/10.1016/S0140-6736(20)32594-0)
- WHO. *Global Nutrition Targets 2025: Anaemia Policy Brief*. Geneva: World Health Organization; 2014. Accessed January 26, 2024. <https://www.who.int/publications-detail-redirect/WHO-NMH-NHD-14.4>
- Avni T, Bieber A, Grossman A, Green H, Leibovici L, Gafter-Gvili A. The safety of intravenous iron preparations: systematic review and meta-analysis. *Mayo Clin Proc*. 2015;90(1):12–23. <https://doi.org/10.1016/j.mayocp.2014.10.007>
- Wolf M, Koch TA, Bregman DB. Effects of iron deficiency anemia and its treatment on fibroblast growth factor 23 and phosphate homeostasis in women. *J Bone Miner Res*. 2013;28(8):1793–1803. <https://doi.org/10.1002/jbmr.1923>
- Zoller H, Schaefer B, Glodny B. Iron-induced hypophosphatemia: an emerging complication. *Curr Opin Nephrol Hypertens*. 2017;26(4):266–275. <https://doi.org/10.1097/MNH.0000000000000329>
- Schaefer B, Tobiasch M, Viveiros A, et al. Hypophosphataemia after treatment of iron deficiency with intravenous ferric carboxymaltose or iron isomaltoside—a systematic review and meta-analysis. *Br J Clin Pharmacol*. 2021;87(5):2256–2273. <https://doi.org/10.1111/bcp.14643>
- Vilaca T, Velmurugan N, Smith C, Abrahamsen B, Eastell R. Osteomalacia as a complication of intravenous iron infusion: a systematic review of case reports. *J Bone Miner Res*. 2022;37(6):1188–1199. <https://doi.org/10.1002/jbmr.4558>
- Glaspay JA, Wolf M, Strauss WE. Intravenous iron-induced hypophosphatemia: an emerging syndrome. *Adv Ther*. 2021;38(7):3531–3549. <https://doi.org/10.1007/s12325-021-01770-2>
- Klein K, Asaad S, Econs M, Rubin JE. Severe FGF23-based hypophosphataemic osteomalacia due to ferric carboxymaltose administration. *BMJ Case Rep*. 2018;2018:bcr-2017-222851. <https://doi.org/10.1136/bcr-2017-222851>
- Schaefer B, Tobiasch M, Wagner S, et al. Hypophosphatemia after intravenous iron therapy: comprehensive review of clinical findings and recommendations for management. *Bone*. 2022;154:116202. <https://doi.org/10.1016/j.bone.2021.116202>
- Shuhart CR, Yeap SS, Anderson PA, et al. Executive summary of the 2019 ISCD position development conference on monitoring treatment, DXA cross-calibration and least significant change, spinal cord injury, peri-prosthetic and orthopedic bone health, transgender medicine, and pediatrics. *J Clin Densitom*. 2019;22(4):453–471. <https://doi.org/10.1016/j.jocd.2019.07.001>
- Whittier DE, Boyd SK, Burghardt AJ, et al. Guidelines for the assessment of bone density and microarchitecture *in vivo* using high-resolution peripheral quantitative computed tomography. *Osteoporos Int*. 2020;31(9):1607–1627. <https://doi.org/10.1007/s00198-020-05438-5>
- Bartosik M, Simon A, Strahl A, Oheim R, Amling M, Schmidt FN. Comparison of motion grading in 1,000 patients by first- and second-generation HR-pQCT: a propensity score matched cohort study. *Calcif Tissue Int*. 2023;113(6):597–608. <https://doi.org/10.1007/s00223-023-01143-7>
- Manske SL, Davison EM, Burt LA, Raymond DA, Boyd SK. The estimation of second-generation HR-pQCT from first-generation HR-pQCT using *in vivo* cross-calibration. *J Bone Miner Res*. 2017;32(7):1514–1524. <https://doi.org/10.1002/jbmr.3128>
- Burt LA, Liang Z, Sajobi TT, Hanley DA, Boyd SK. Sex- and site-specific normative data curves for HR-pQCT. *J Bone Miner Res*. 2016;31(11):2041–2047. <https://doi.org/10.1002/jbmr.2873>
- Hansen S, Shanbhogue V, Folkestad L, Nielsen MMF, Brixen K. Bone microarchitecture and estimated strength in 499 adult Danish women and men: a cross-sectional, population-based high-resolution peripheral quantitative computed tomographic study on peak bone structure. *Calcif Tissue Int*. 2014;94(3):269–281. <https://doi.org/10.1007/s00223-013-9808-5>
- Schmidt FN, Delsmann J, Yazigi B, Beil FT, Amling M, Oheim R. Approaching virtual osteoid volume estimation and in-depth tissue characterization in patients with tumor-induced Osteomalacia. *J Bone Miner Res*. 2024;39(2):116–129. <https://doi.org/10.1093/jbmr/zjae008>
- von Brackel FN, Oheim R. Iron and bones: effects of iron overload, deficiency and anemia treatments on bone. *JBMR Plus*. 2024;8(8):ziae064. <https://doi.org/10.1093/jbmrpl/ziae064>
- Schmidt FN, Zimmermann EA, Walsh F, et al. On the origins of fracture toughness in advanced Teleosts: how the swordfish Sword's bone structure and composition allow for slashing under water to kill or stun prey. *Adv Sci*. 2019;6(12):1900287. <https://doi.org/10.1002/advs.201900287>

20. Schmidt FN, Delsmann MM, Mletzko K, et al. Ultra-high matrix mineralization of sperm whale auditory ossicles facilitates high sound pressure and high-frequency underwater hearing. *Proc Biol Sci*. 2018;285(1893):20181820. <https://doi.org/10.1098/rspb.2018.1820>
21. Fratzl-Zelman N, Hartmann MA, Gamsjaeger S, et al. Bone matrix mineralization and response to burosumab in adult patients with X-linked hypophosphatemia: results from the phase 3, single-arm international trial. *J Bone Miner Res*. 2022;37(9):1665–1678. <https://doi.org/10.1002/jbmr.4641>
22. Jan de Beur SM, Miller PD, Weber TJ, et al. Burosumab for the treatment of tumor-induced osteomalacia. *J Bone Miner Res*. 2021;36(4):627–635. <https://doi.org/10.1002/jbmr.4233>
23. Amarnani R, Travis S, Javaid MK. Novel use of burosumab in refractory iron-induced FGF23-mediated hypophosphataemic osteomalacia. *Rheumatology (Oxford)*. 2020;59(8):2166–2168. <https://doi.org/10.1093/rheumatology/kez627>